

Time-resolved structural analysis

Visualization of Atomic-Scale
Motions in Materials via
Femtosecond X-Ray Scattering
Techniques

Aaron M. Lindenberg,^{1,2} Steven L. Johnson,³
and David A. Reis^{2,4}

¹Department of Materials Science and Engineering, Stanford University, Stanford, California 94305; email: aaronl@stanford.edu

²Department of Photon Science, Stanford University and SLAC National Accelerator Laboratory, Menlo Park, California 94025

³Institute for Quantum Electronics, Physics Department, ETH Zürich, 8093 Zürich, Switzerland

⁴Department of Applied Physics, Stanford University, Stanford, California 94305

Sébastien Pillet

Time-resolved structural analysis: probing condensed matter in motion

Keywords: time-resolved X-ray scattering

Introduction

Without any doubt, one of the most fundamental properties of a solid is its crystallographic structure. A thorough understanding of the physical properties of condensed matter requires a detailed mapping of the atomic structure and its dynamics over multiple length scales and different time scales. Several methods may provide a detailed description of the structural organization of matter, such as elastic scattering/diffraction of X-rays, neutrons or electrons, X-ray absorption spectroscopies (EXAFS and XANES), and magnetic resonance spectroscopies (NMR, NQR). X-ray diffraction is nowadays routinely applied through laboratory diffractometer setups run by X-ray tube or rotating anode sources, whereas synchrotron radiation facilities, owing to their wavelength tunability and high spatial and temporal coherence, afford additional possibilities of unique experiments such as resonant X-ray diffraction or coherent scattering.

1. INTRODUCTION

Atomic-scale motions in materials occur across a vast range of timescales and length scales. Our understanding of these processes is shaped by our ability to probe them, and over the past century, a range of approaches have been adapted to try to visualize how atoms are moving. For example, in the frequency domain, optical techniques such as infrared or Raman spectroscopy are sensitive to vibrational degrees of freedom and can extract important structural information. Over the last several decades, significant efforts have been made to go beyond these more indirect approaches and to develop means to reconstruct the structure of materials at atomic-scale resolution as they are evolving. This means extending basic techniques such as X-ray crystallography, as often applied to measure frozen-in structures of biologically relevant molecules, to extract the intermediate states and mechanistic pathways that the molecules pass through as they transform (i.e., not just reactant and product states) (1). In the realm of materials science and solid-state physics on which this review is focused, direct information concerning how atoms are moving and how unit cells are deforming and reconfiguring can be obtained through these approaches, despite the fact that the timescale for these dynamics can be as fast as a few tens of femtoseconds (10^{-15} s), comparable to the period of the highest-frequency optical phonons. For example, the original fruit fly of femtosecond X-ray experiments concerned the study of bismuth crystals, where time-dependent measurements of the X-ray structure factor enable direct measurement of the unit cell deformations associated with the A_{1g} phonon mode and the Peierls distorted structure (2, 3). Since these early days, sources have improved by many orders of magnitude in brightness (4), and the range of materials systems that can be studied and the information that may be gleaned have been extended to encompass a vastly larger phase space.

Galloping Horse Problem

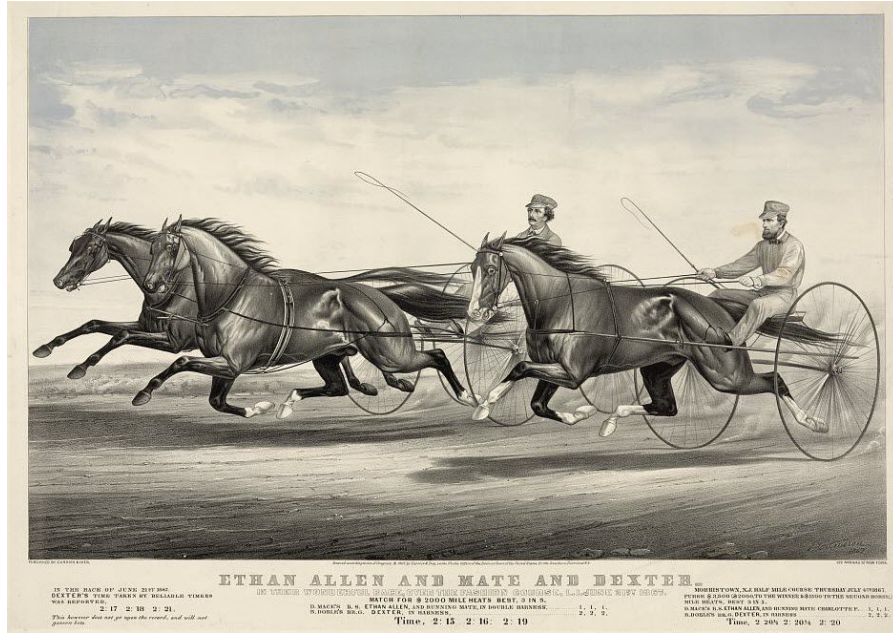


"Baronet"
by George Stubbs, 1794

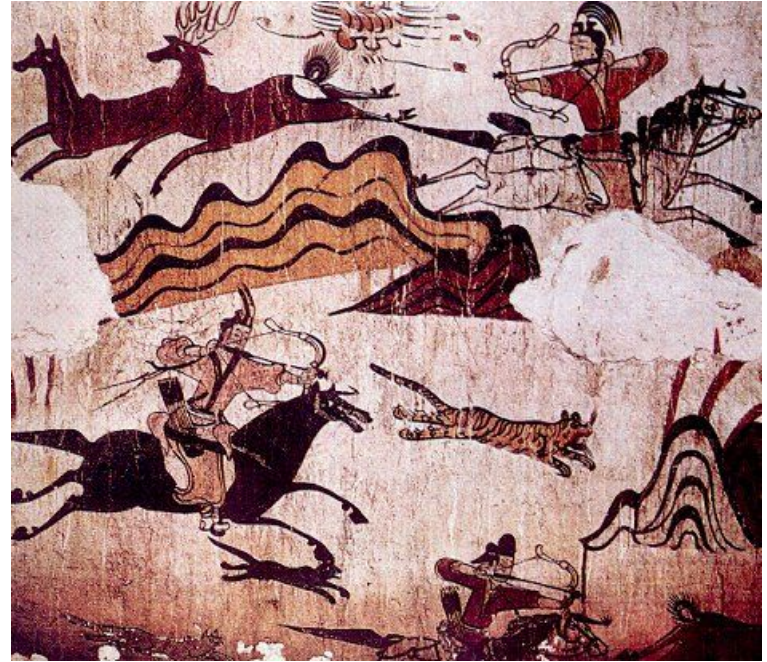


"The 1821 Derby at Epsom"
by Théodore Géricault, 1821

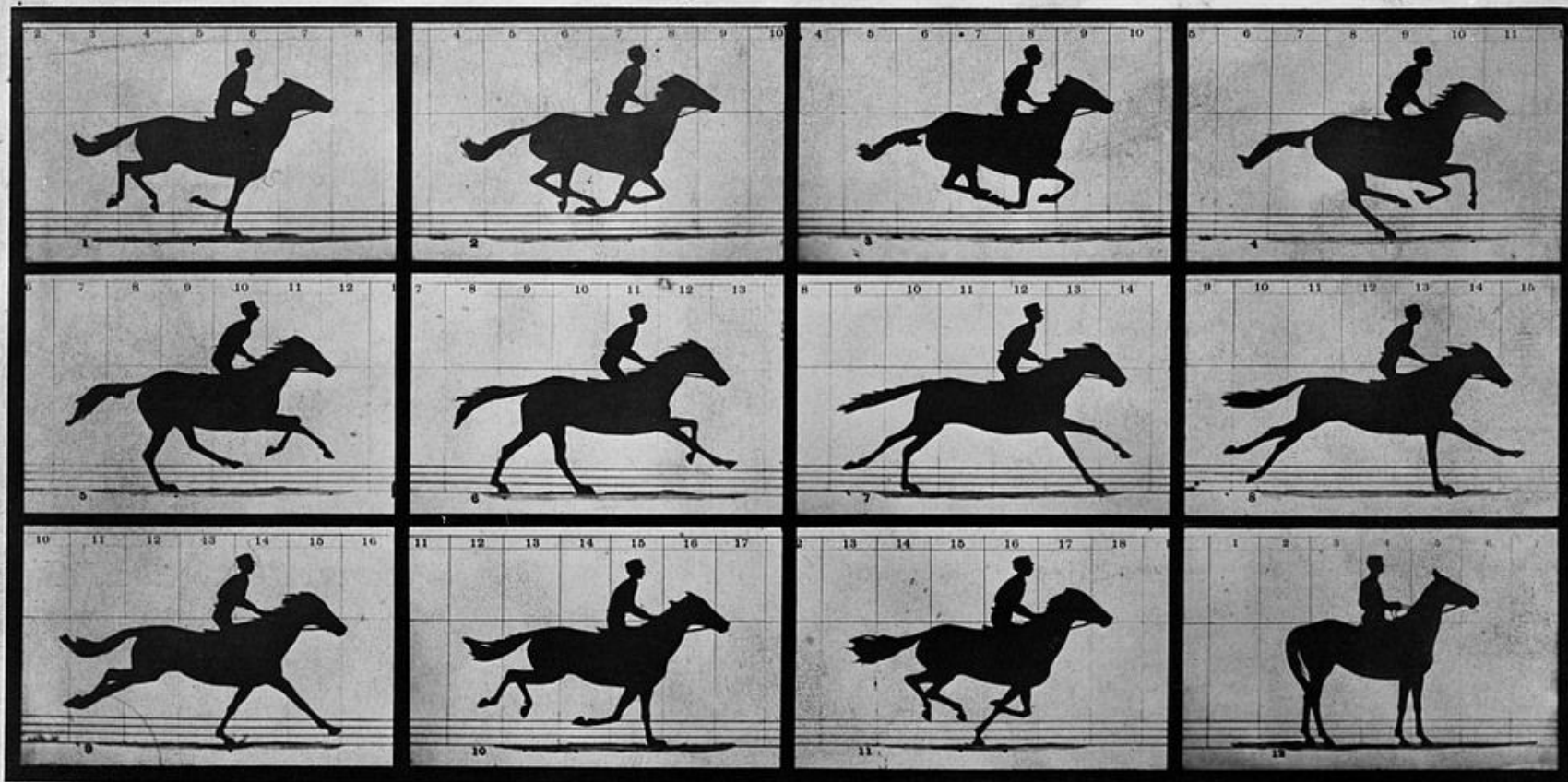
Galloping Horse Problem



*"Ethan Allen and Mate and Dexter"
by John Cameron, 1828*



JYM458, ~5th Century.



Copyright, 1878, by MUYBRIDGE.

MORSE'S Gallery, 417 Montgomery St., San Francisco.

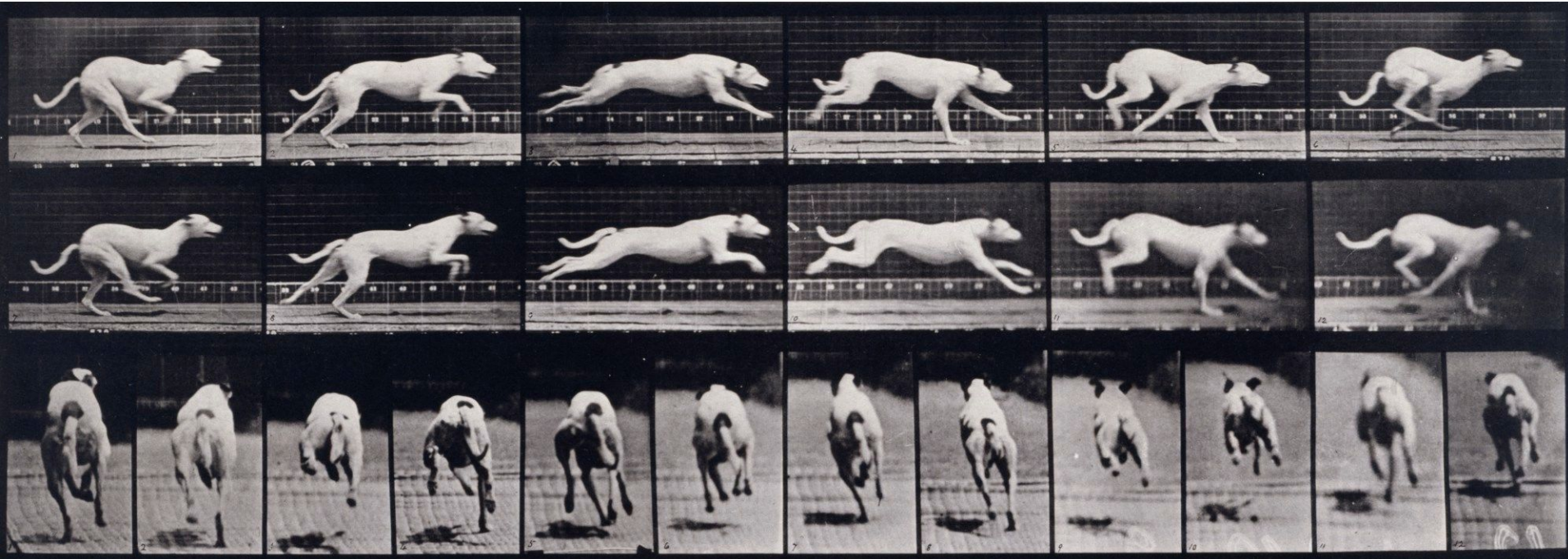
THE HORSE IN MOTION.

Illustrated by
MUYBRIDGE.

AUTOMATIC ELECTRO-PHOTOGRAPH.

"SALLIE GARDNER," owned by LELAND STANFORD; running at a 1.40 gait over the Palo Alto track, 19th June, 1878.

The negatives of these photographs were made at intervals of twenty-seven inches of distance, and about the twenty-fifth part of a second of time; they illustrate consecutive positions assumed in each twenty-seven inches of progress during a single stride of the mare. The vertical lines were twenty-seven inches apart; the horizontal lines represent elevations of four inches each. The exposure of each negative was less than the two-thousandth part of a second.



Brief early history of the time-resolving studies.

- 1872–1878 Eadweard Muybridge, *The Man Who Stopped Time*, solved Galloping Horse Problem. The project cost was about \$50,000.
- 1899 Abraham and Lemoine measured the duration of light emitted by the spark by using light-path varying measurement. The lifetime was <10 ns.
- 1917 first electric stroboscope was invented, camera frame rates reached up to ~ 1 k fps.
- 1950 Norrish and Porter demonstrated the 1st real pump-probe experiment. Flash lamps is used to excite photochemical reactions and probed them spectroscopically with varying delays in μs – ms range. (Nobel prize for chemistry in 1967)

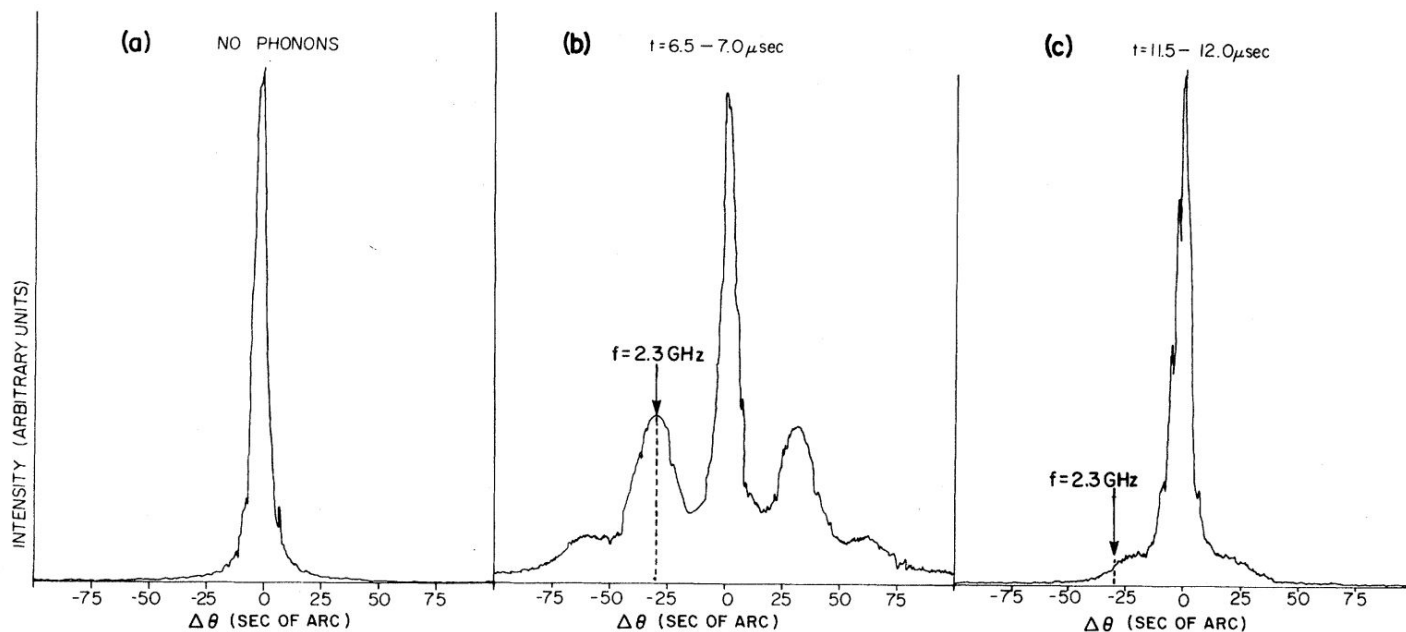
Brief history of the short-pulse generation.

- 1917, Albert Einstein established the theoretical foundations for the laser and maser
- 1950, Alfred Kastler (Nobel prize winner, 1966) proposed optical pumping method.
- 1952, Brossel, Kastler, and Winter experimentally demonstrated optical pumping method.
- 1960, Maiman realize the 1st laser (ruby). The laser pulse duration was in μs – ms range.
- 1961, Hellwarth proposed Q-switching laser equipped with Kerr-cell shutter.
- 1964, First (active) mode-locking HeNe laser ($>\sim 1$ ns) demonstrated by Hargrove, Fork, and Pollack.
- 1965, First (passive) mode-locking laser (Ruby) was demonstrated by Mocker and Collins.
- 1966, passive mode locking of a Nd-glass laser (< 1 ns), later Nd-YAG laser obtained pulse duration of 10 ps
- 1967, Stephen E. Harris *et al.* demonstrated spontaneous parametric down-conversion. (OPG)
- 1974, Shank and Ippen realized tunable broad gain dye laser which has a pulse duration of < 1 ps
- 1987, Fork et al. reported group velocity dispersion compensation technique to achieve 6 fs pulse.
- 1987, McPherson et al. generates high harmonic emission.
- 1991, Spence, Kean, and Sibbett demonstrated spontaneous dynamic mode locking laser based on Ti:sapphire
- 1994, Zhou *et al.* demonstrated Ti:sapphire laser pulse of 8 fs duration using group velocity dispersion compensation.

Brief history of the ultrafast x-ray sciences.

InSb (0 0 4)
(004) BRAGG REFLECTION

Phys. Rev. B, **27** 2264–2277, (1983)



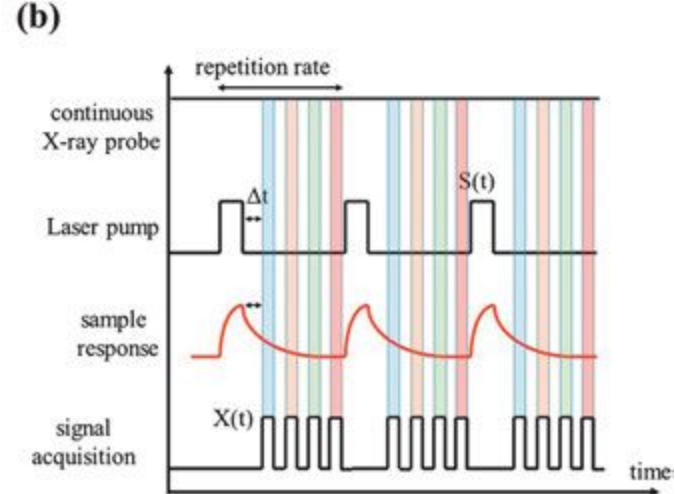
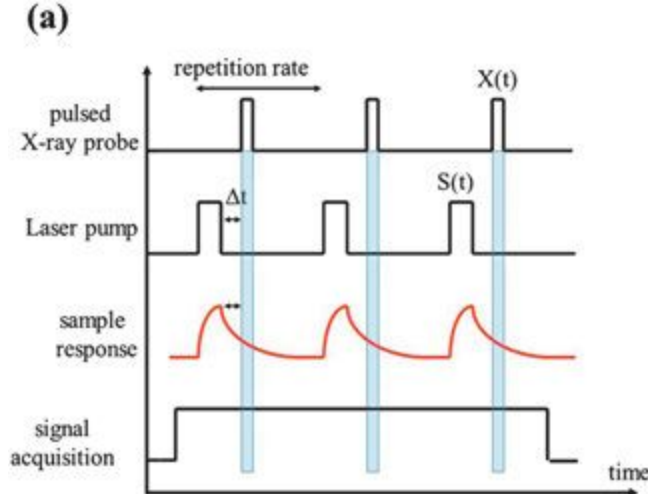
Brief history of the ultrafast x-ray sciences.

Time-resolved x-ray scattering offers:

- Quantitative information on magnitude of coherences,
- Measurement of certain types of couplings,
- Wave vector of coherences.

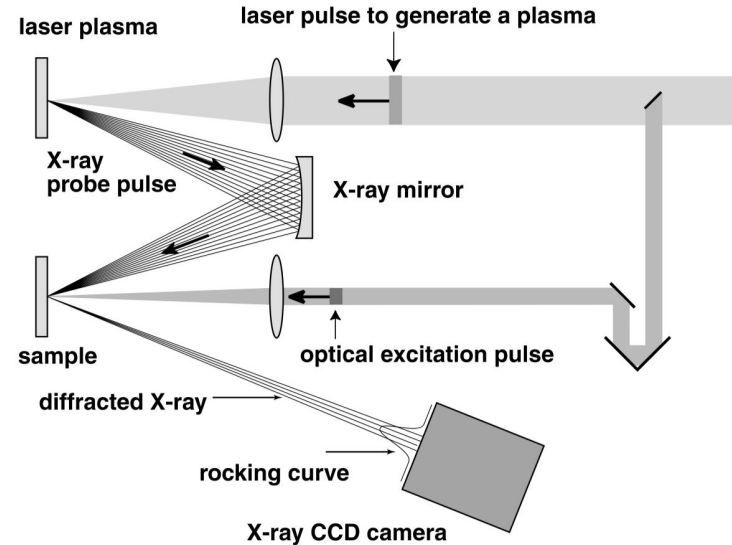
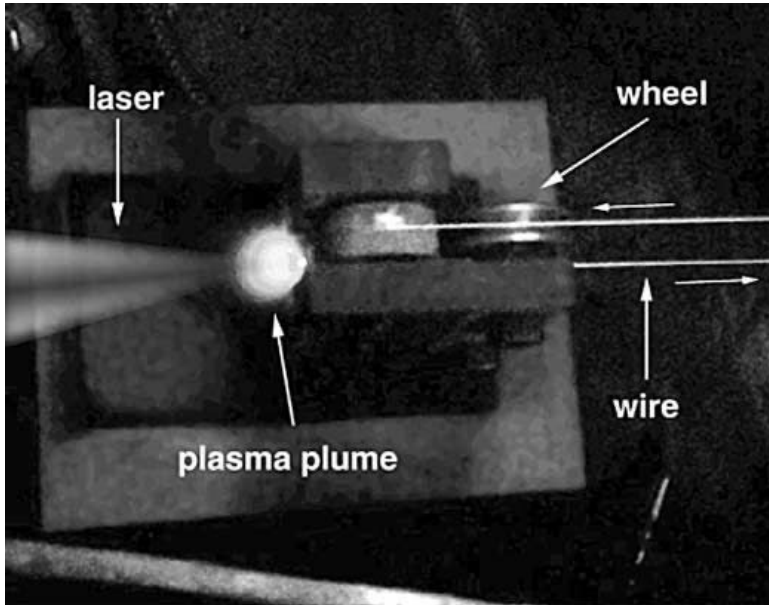
Brief history of the ultrafast x-ray sciences.

- 1989–1993, Ultrashort x-ray pulse from femtosecond laser driven plasma was generated and started to use .
- 1996, ultrafast (\sim ps) streak camera developed and adopted on synchrotrons.



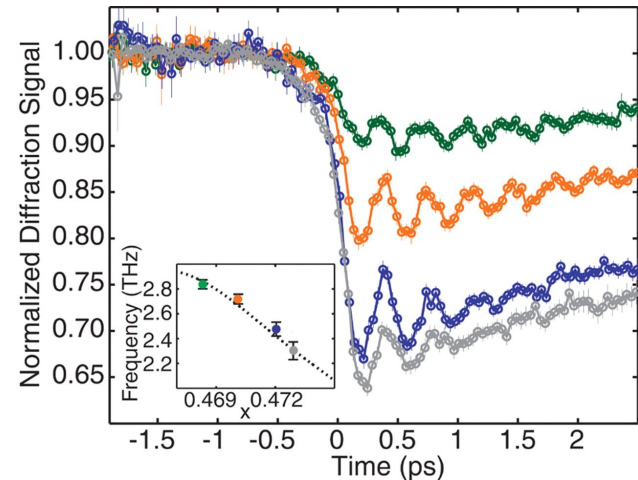
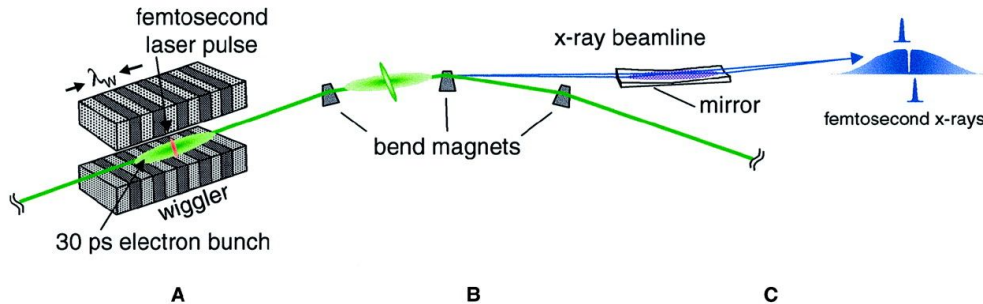
Brief history of the ultrafast x-ray sciences.

- 1989–1993, Ultrashort x-ray pulse from femtosecond laser driven plasma was generated and started to use .
- 1996, ultrafast (\sim ps) streak camera developed and adopted on synchrotrons.

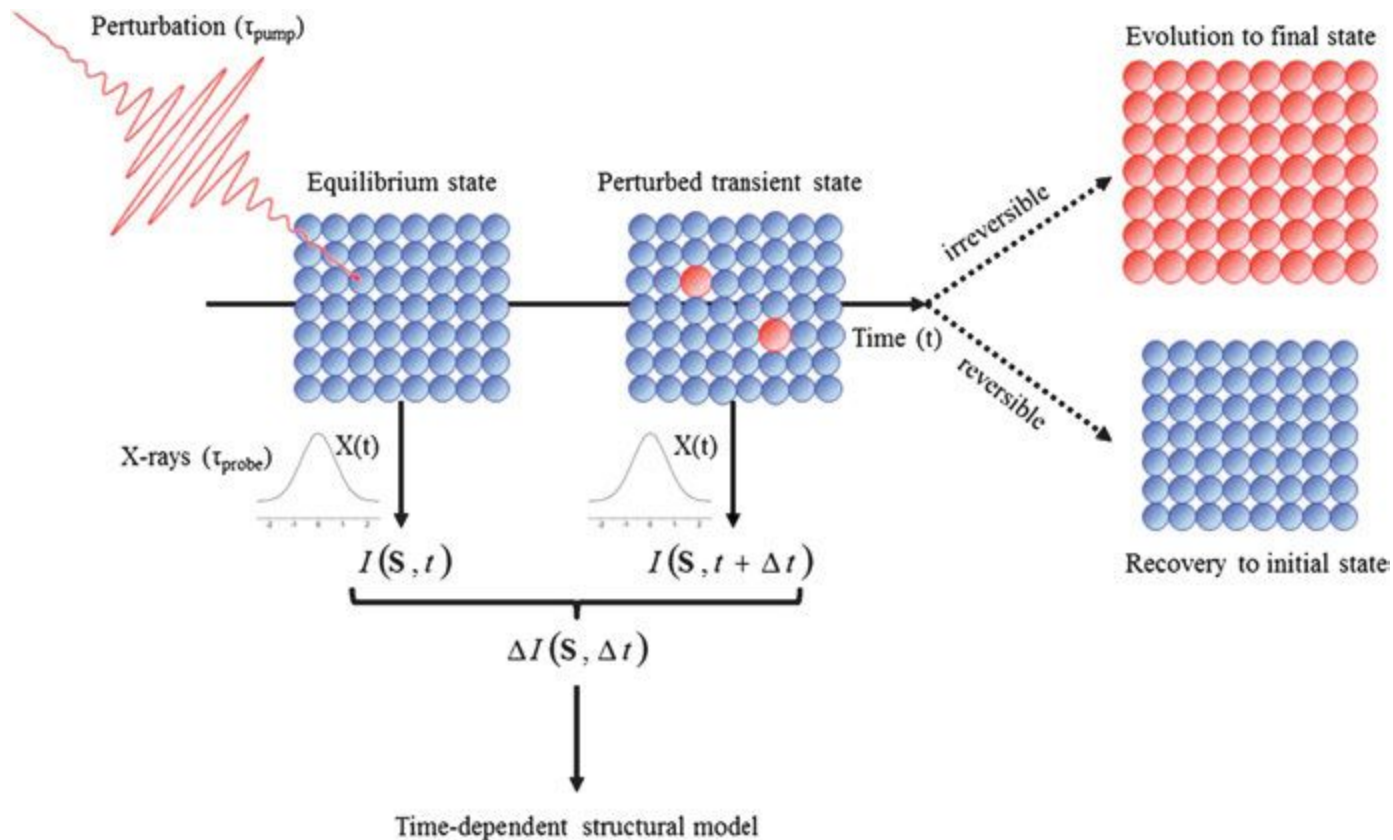


Brief history of the ultrafast x-ray sciences.

- 1996, fs x-ray generation at synchrotron were proposed.
- 2000, Synchrotron based fs x-ray pulse were generated.
- 2007, Pump-probe experiments using fs x-ray pulse based on Linac (at SLAC) were reported. (Optical phonon oscillation on Bismuth)
- 2009, LCLS, the 1st hard x-ray XFEL was commissioned at SLAC



General scheme of a time-resolved experiment



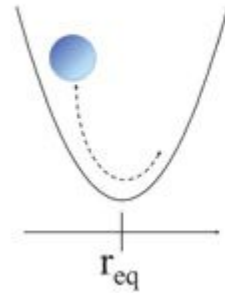
Time-resolved X-ray scattering formalism

$$I(\mathbf{S}) = A(\mathbf{S}) \times A^*(\mathbf{S}) = \sum_{i=1}^{N_{\text{at}}} \sum_{j=1}^{N_{\text{at}}} f_i f_j e^{2i\pi \mathbf{S} \cdot (\mathbf{r}_i - \mathbf{r}_j)}$$

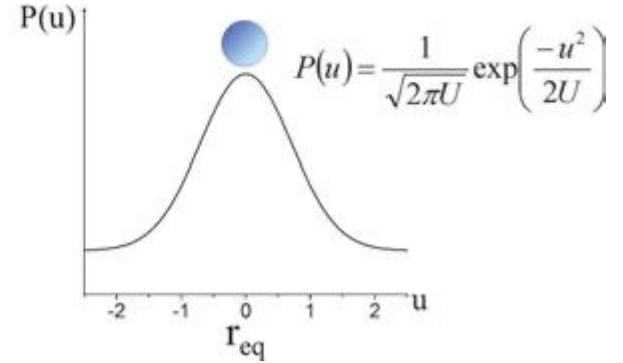
$$T(\mathbf{S}) = e^{-2\pi^2 U S^2} = e^{-8\pi^2 U \frac{\sin^2 \theta}{\lambda^2}} = e^{-B \frac{\sin^2 \theta}{\lambda^2}}$$

$$I(\mathbf{S}, t) = \int_0^\infty X(t) \sum_{i=1}^{N_{\text{at}}} \sum_{j=1}^{N_{\text{at}}} f_i f_j e^{2i\pi \mathbf{S} \cdot (\mathbf{r}_i(t) - \mathbf{r}_j(t))} dt$$

Harmonic potential



Probability density function



(a) Ultrafast incoherent perturbation

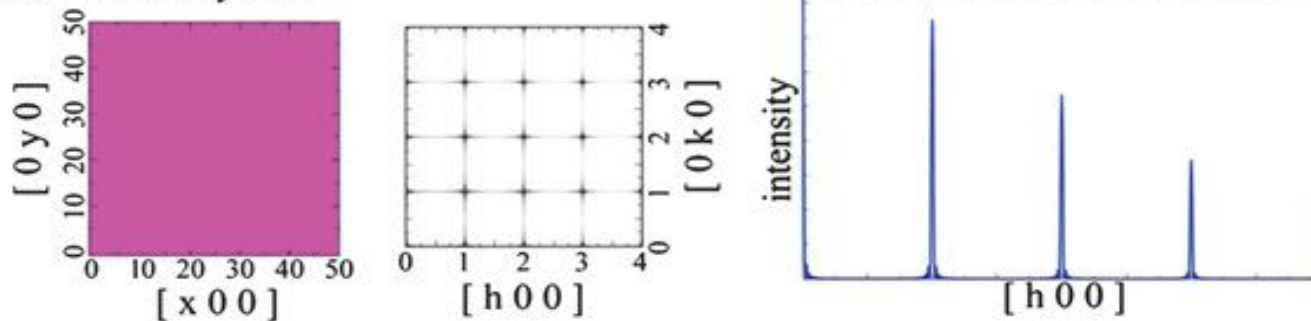


(b) Ultrafast coherent perturbation

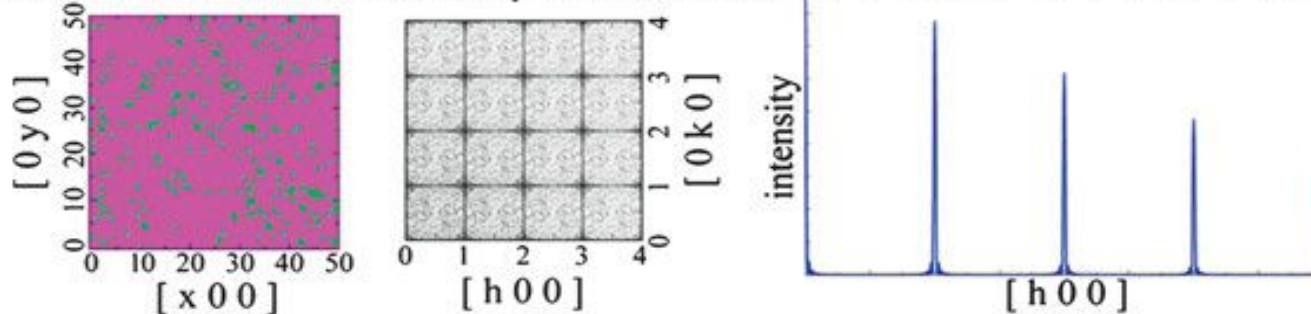


Bragg Peak Intensity & Shape Changes

(a) undistorted crystal

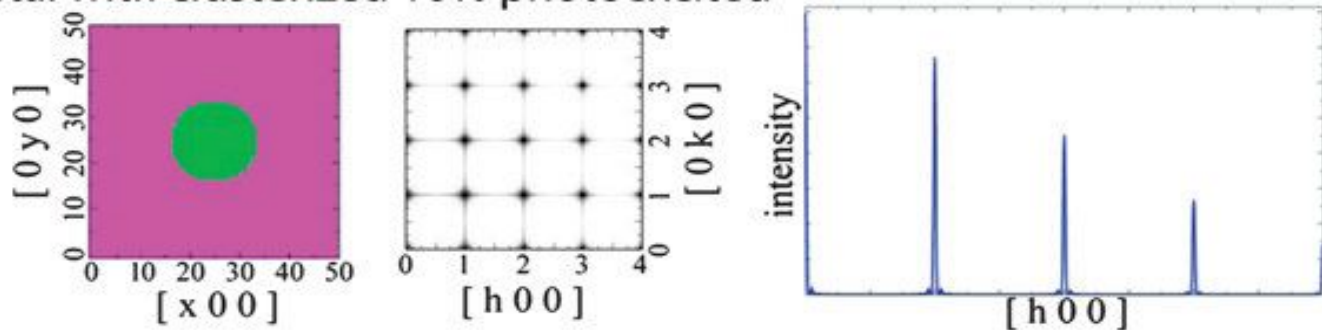


(b) crystal with distributed 10% photoexcited

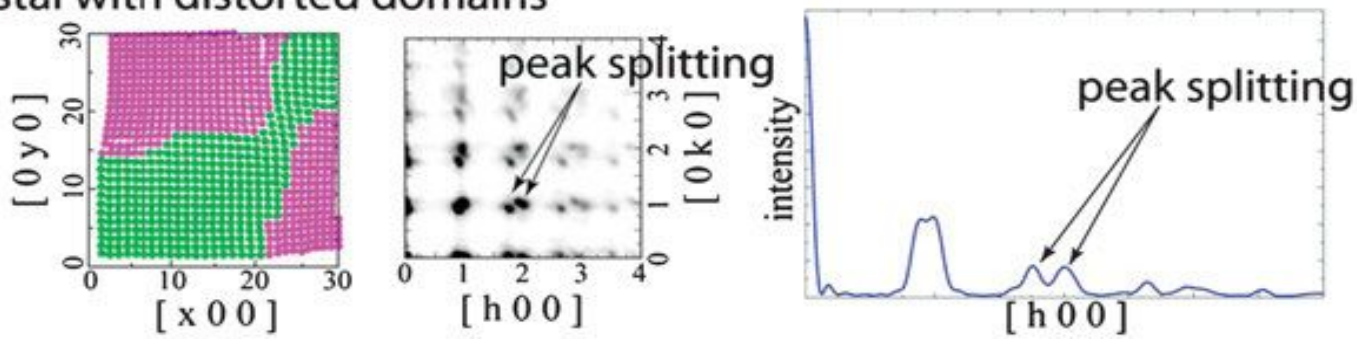


Bragg Peak Intensity & Shape Changes

(c) crystal with clusterized 10% photoexcited

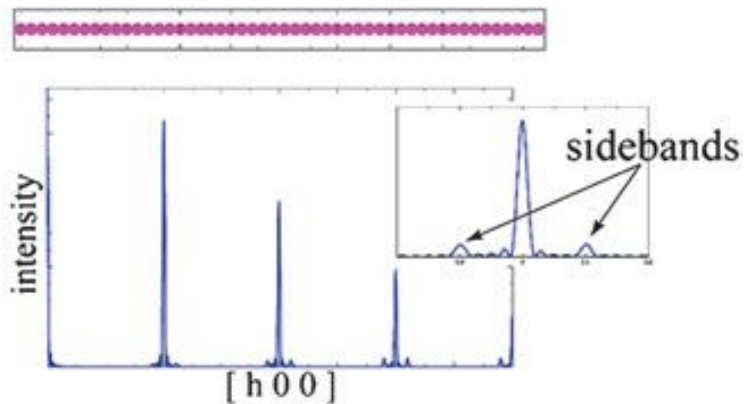
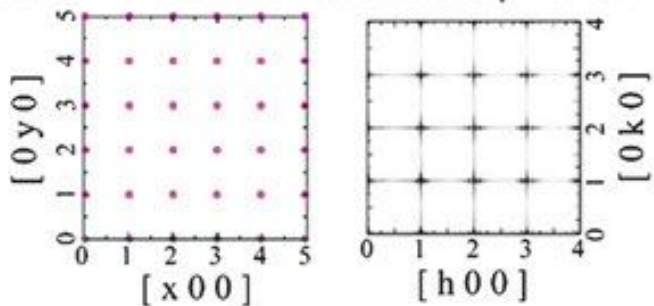


(d) crystal with distorted domains

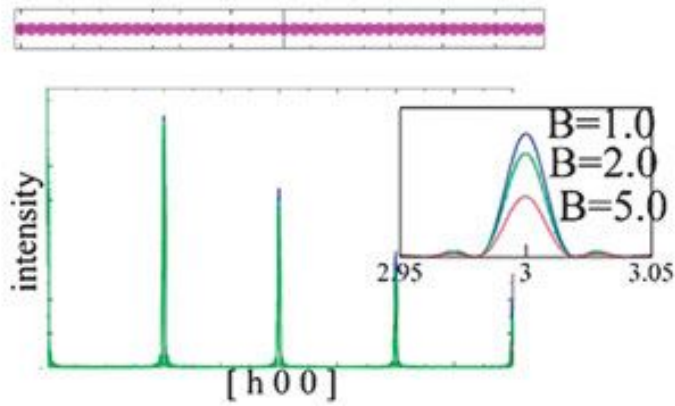
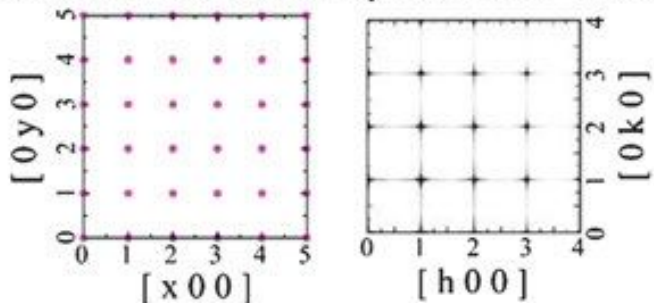


Bragg Peak Intensity & Shape Changes

(e) crystal with coherent acoustic phonon

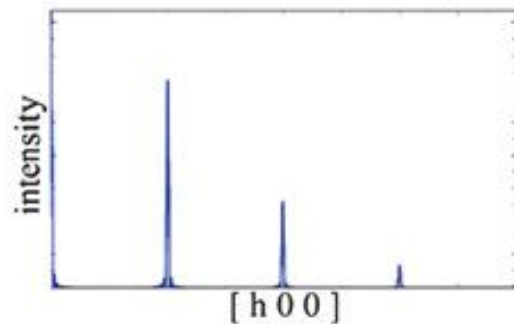
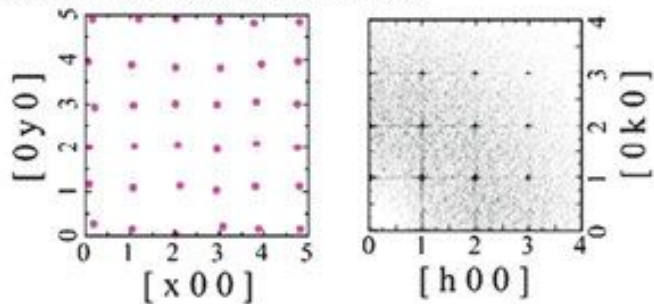


(f) crystal with incoherent phonons (\sim DW)

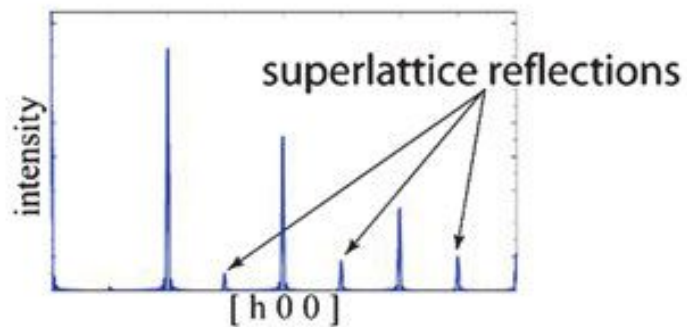
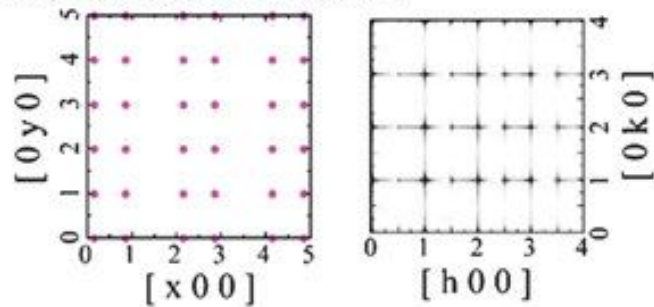


Bragg Peak Intensity & Shape Changes

(g) crystal with static disorder



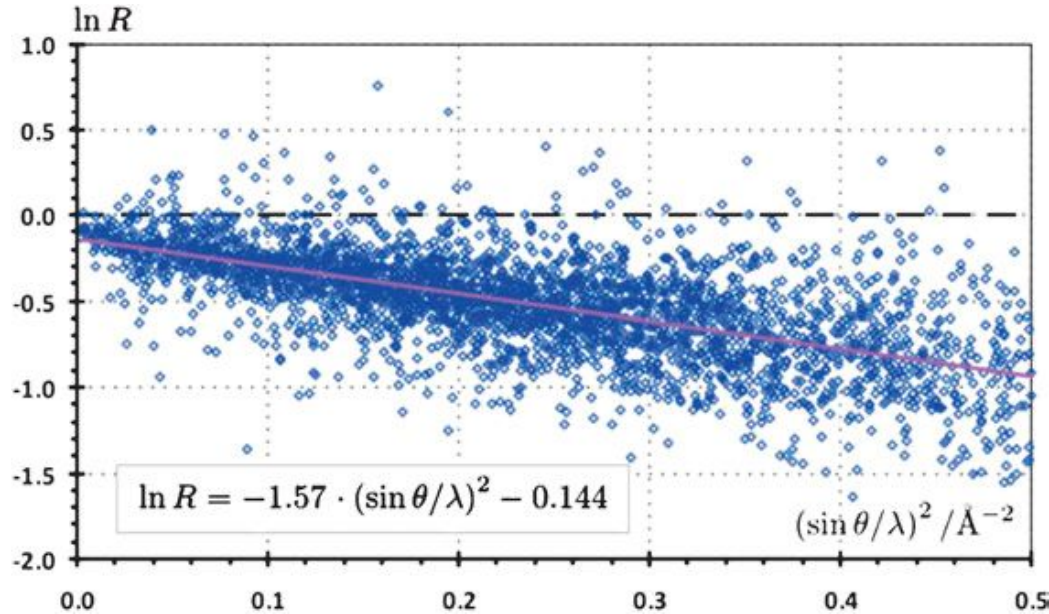
(h) crystal with dimerization



Debye-Waller Parameter Change by Perturbation

$$T(\mathbf{S}) = e^{-2\pi^2 U S^2} = e^{-8\pi^2 U \frac{\sin^2 \theta}{\lambda^2}} = e^{-B \frac{\sin^2 \theta}{\lambda^2}}$$

$$\ln(R) = \ln \left[\frac{I_{\text{on}}(\mathbf{H})}{I_{\text{off}}(\mathbf{H})} \right] = -2\Delta B \frac{\sin^2 \theta}{\lambda^2} + K.$$



Structural Phase Transition: Non-thermal melting

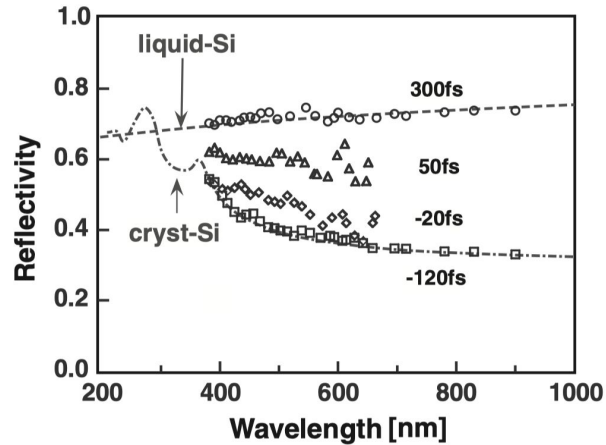


Figure 8. Spectra of the optical reflectivity of silicon. Dash-dotted curve: crystalline silicon. Dashed line: molten silicon. Data points: spectra measured at various time delays between the pump pulse and the optical probe pulse (optical pump/optical probe measurements).

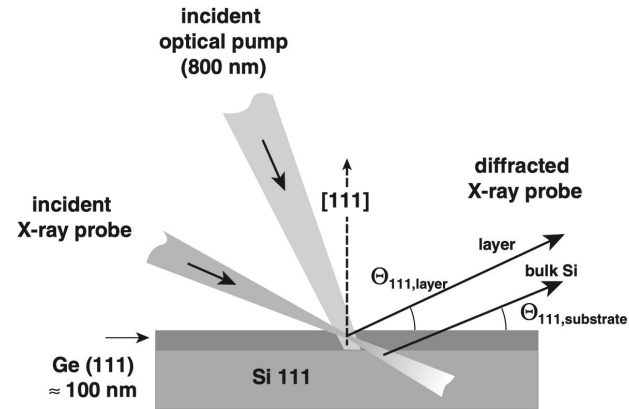


Figure 9. Heteroepitaxial Ge-on-Si samples for optical pump/x-ray probe measurements indicating the selective optical pumping and x-ray probing of the Ge layer.

Structural Phase Transition: Non-thermal melting

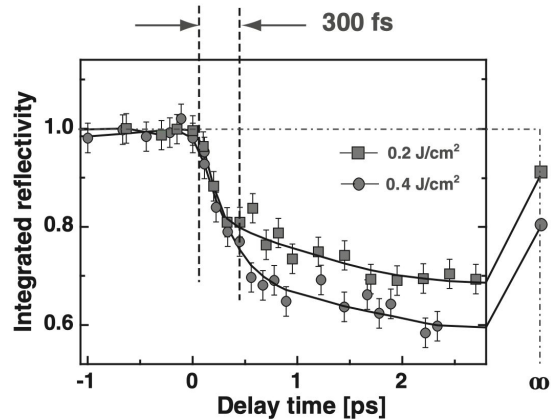
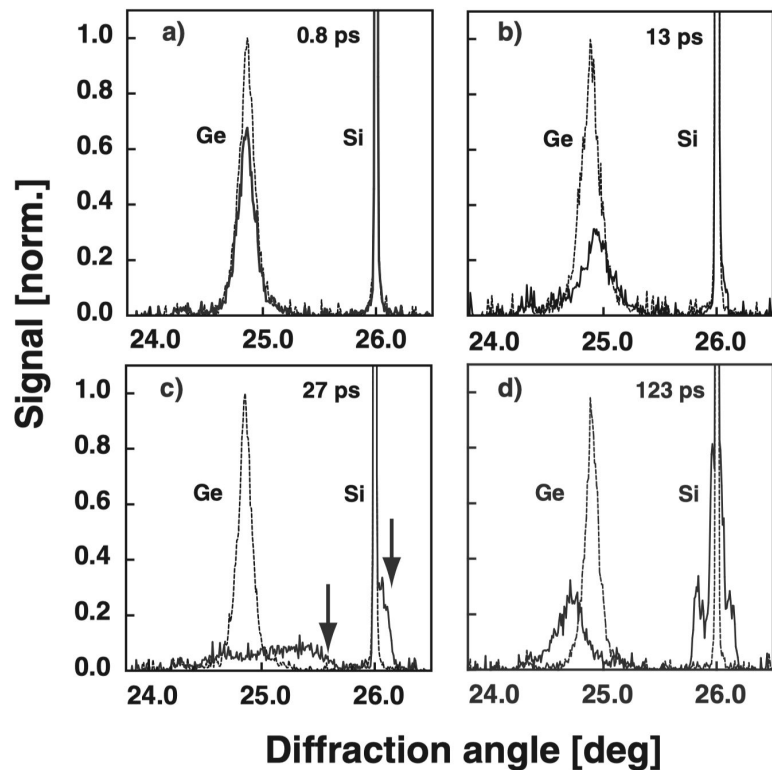
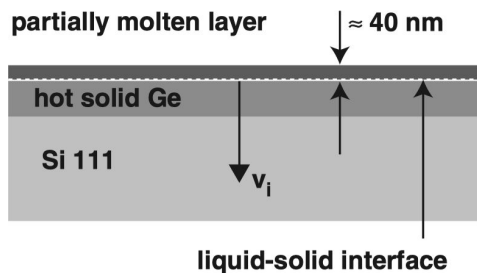


Figure 10. X-ray diffraction from the (111) lattice planes of Ge versus time delay for two different energy fluences of the pump pulse ($\lambda = 800$ nm).



Coherent & Incoherent Lattice Vibration

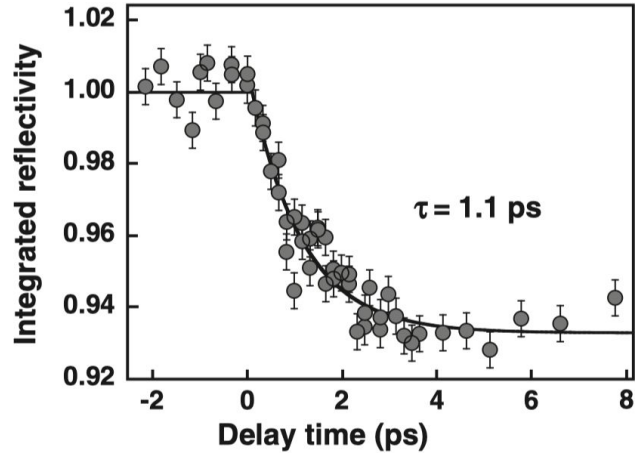
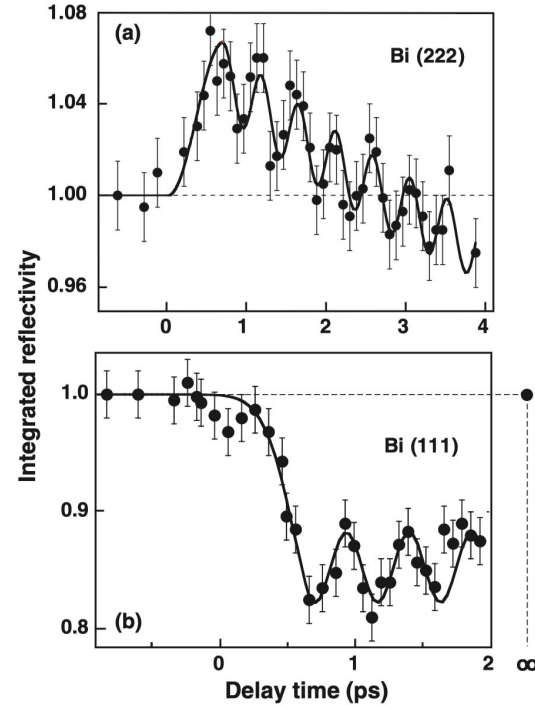
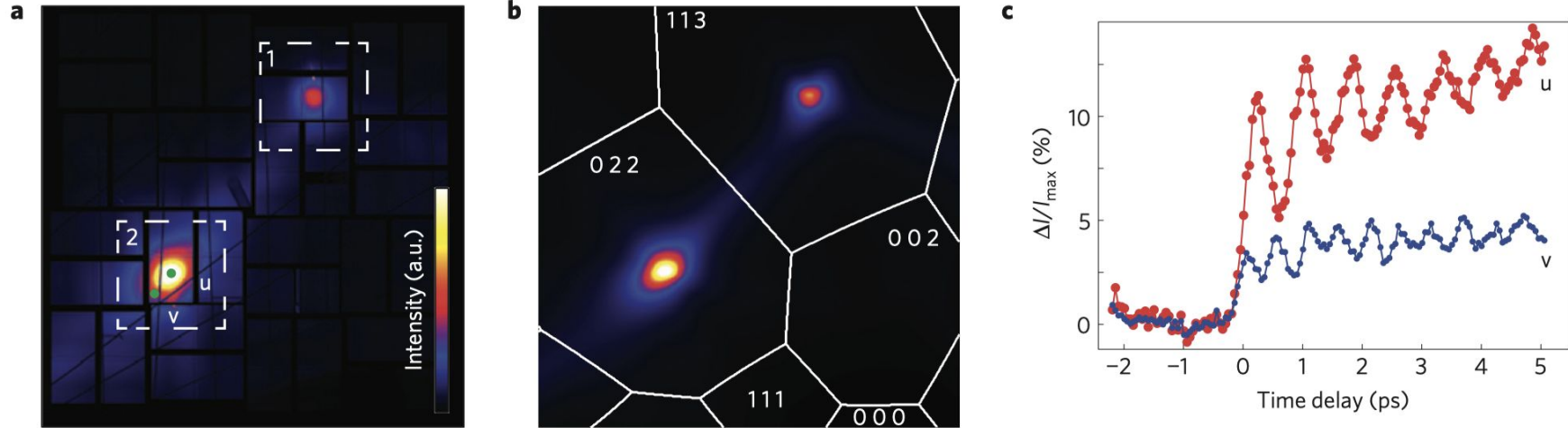


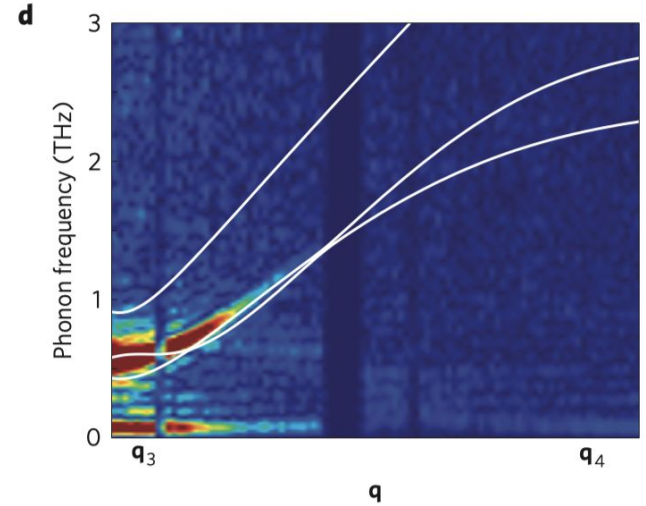
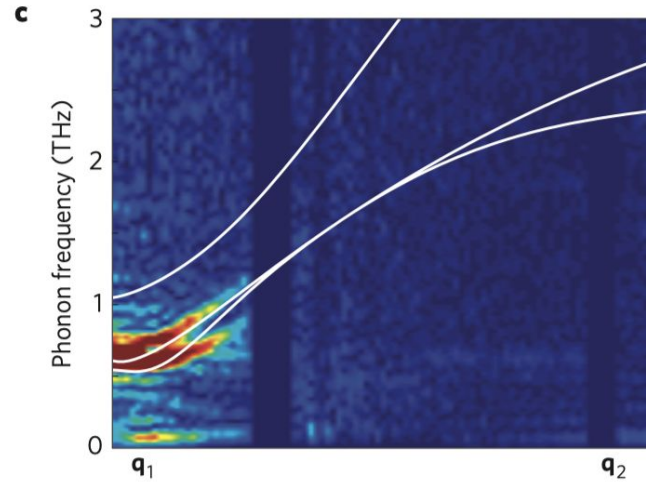
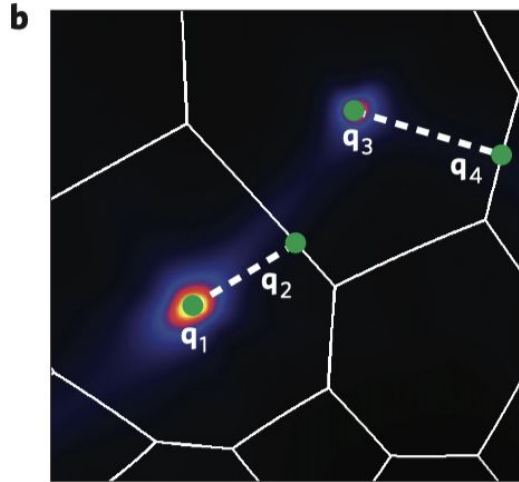
Figure 19. X-ray diffraction from the (400) lattice planes of Ge plotted versus time for weak laser excitation (below the melting threshold). A (111) Ge-Si heteroepitaxial sample.



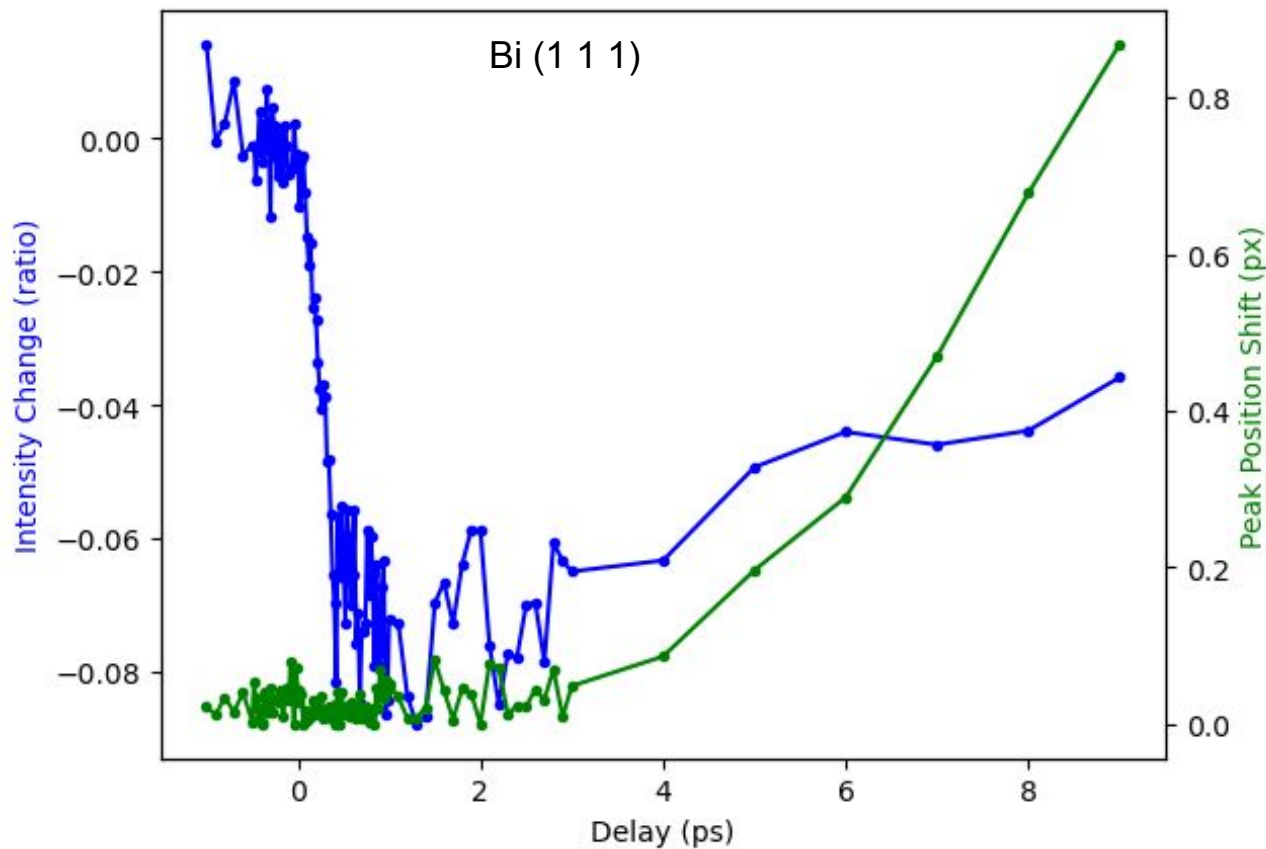
Coherent & Incoherent Lattice Vibration



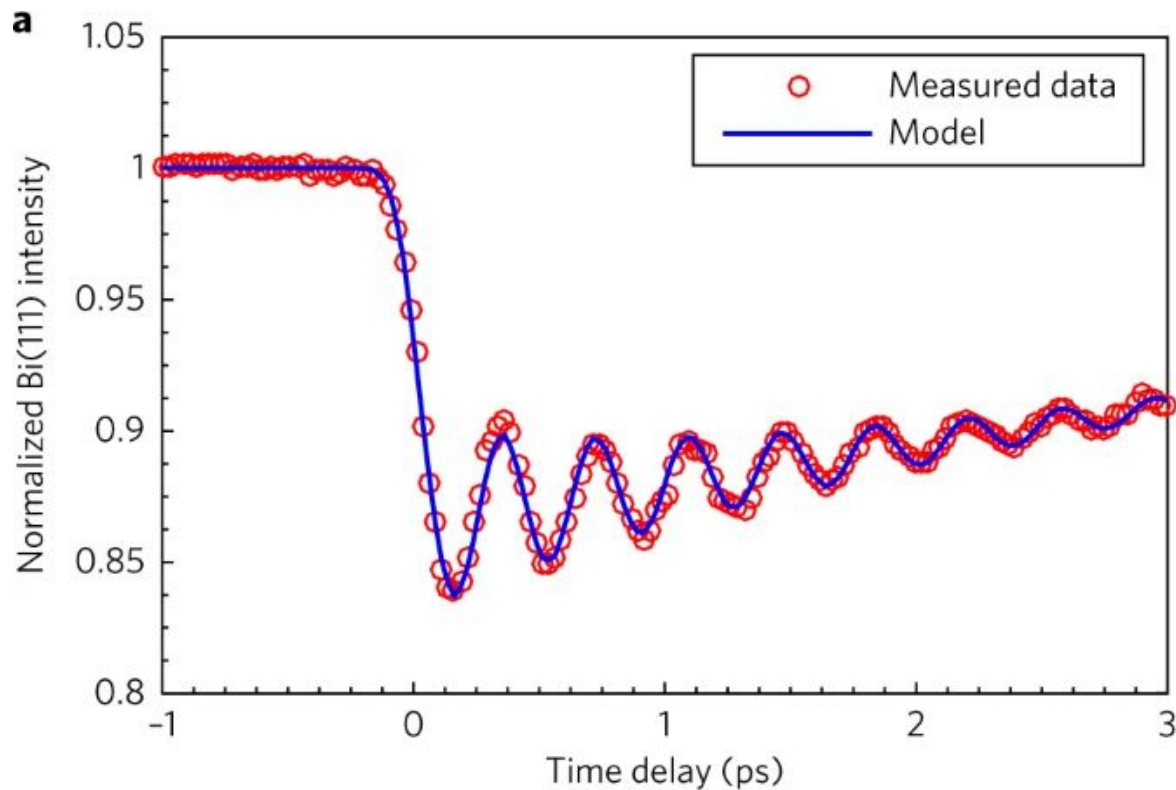
Coherent & Incoherent Lattice Vibration



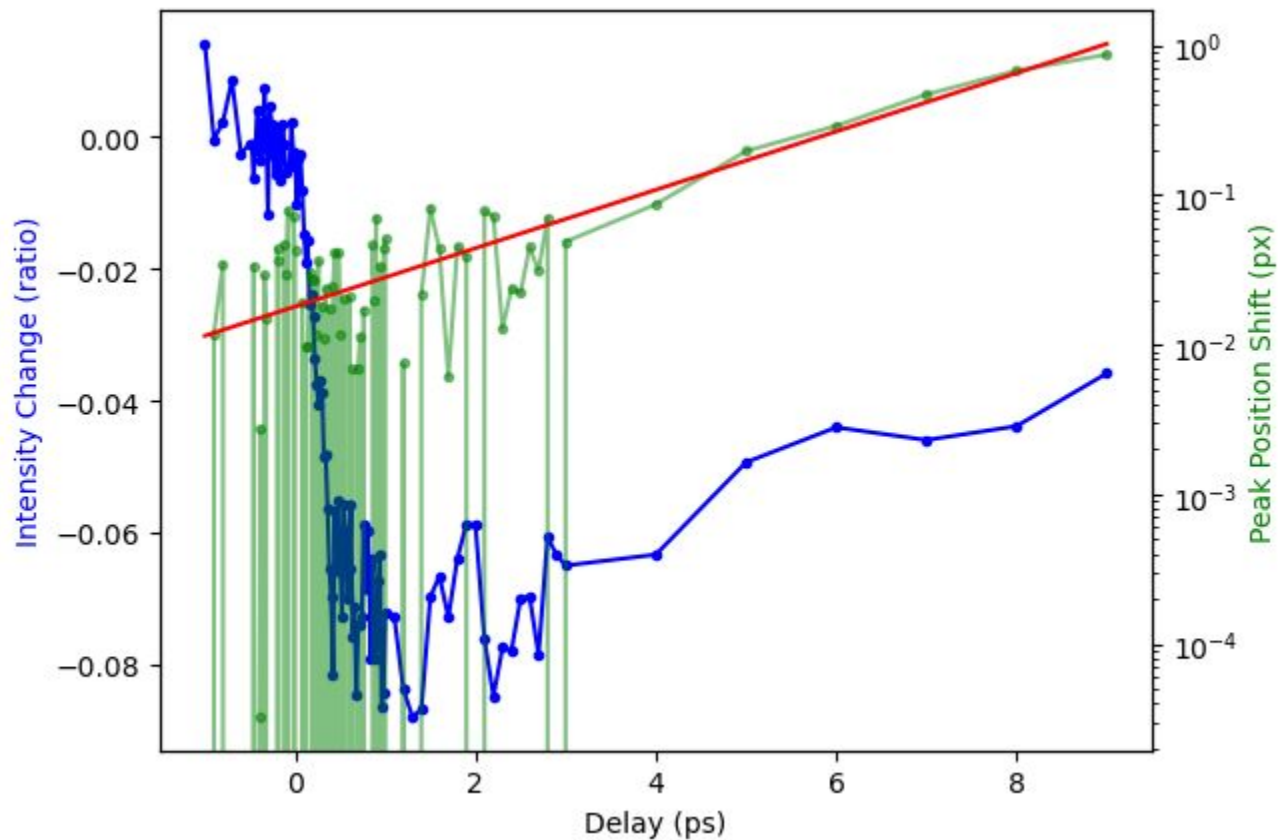
Bragg Peak Shift by Lattice Expansion



Bragg Peak Shift by Lattice Expansion

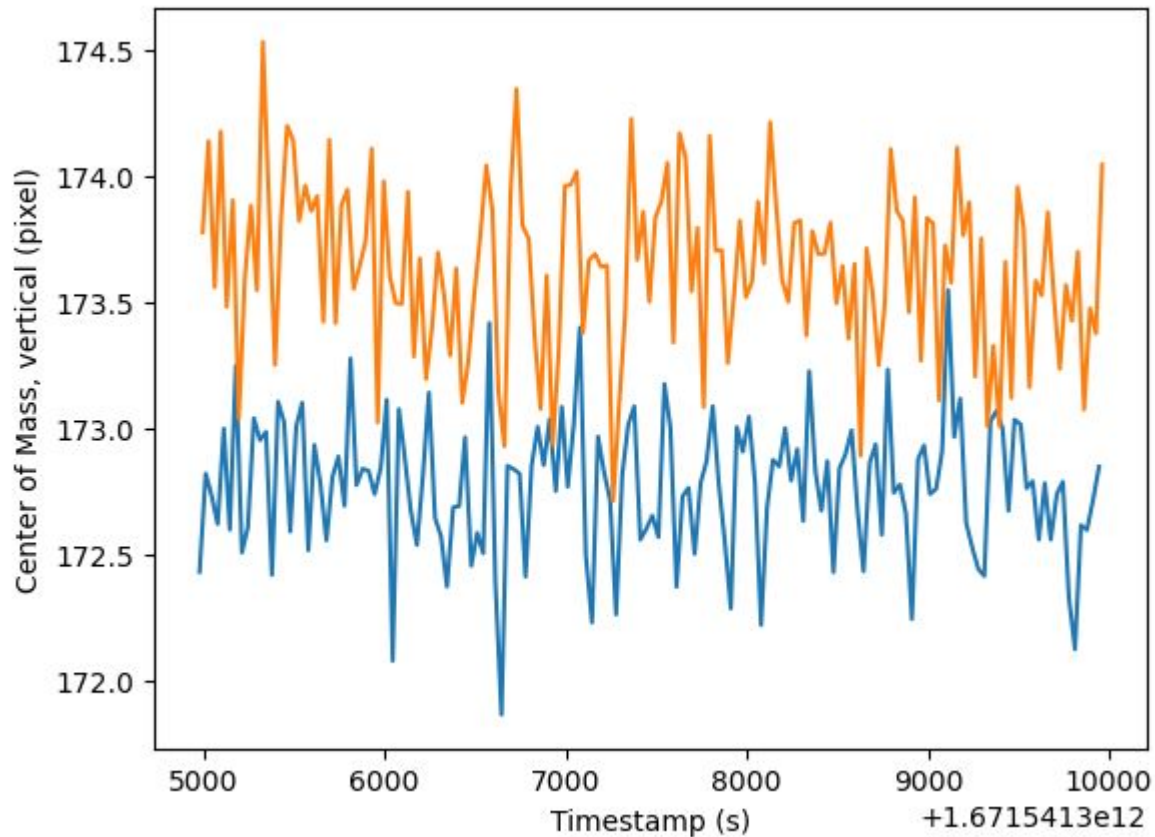


Bragg Peak Shift by Lattice Expansion



Bragg Peak Shift by Lattice Expansion

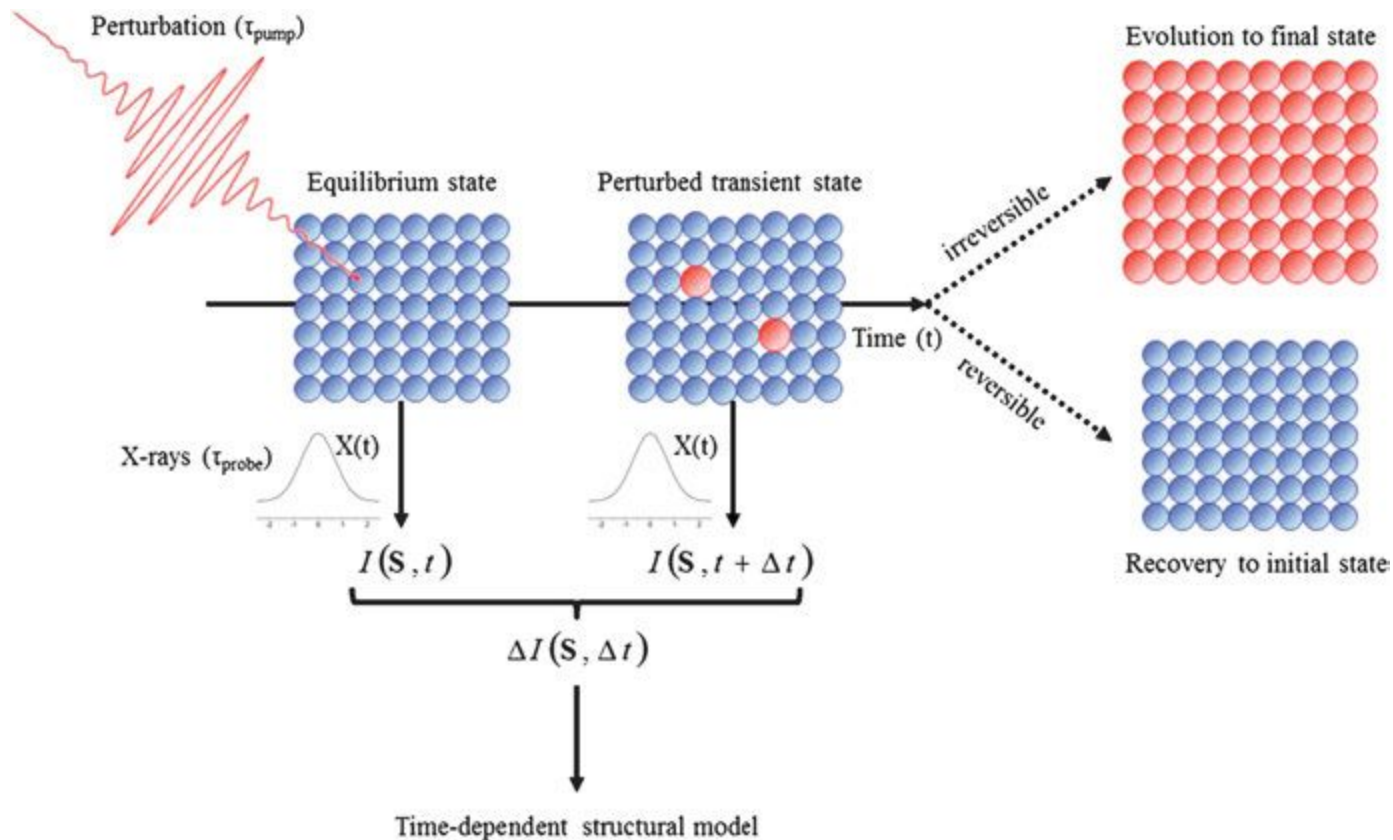
delay=+9ps



SHOT-BY-SHOT TIMING MEASUREMENTS

Because pump and probe pulses are typically generated by independent sources at X-ray FELs, there is often significant timing jitter/fluctuations (of the order of hundreds of femtoseconds). In this situation, auxiliary diagnostic experiments are often used to measure precisely the timing difference between particular pairs of pulses, which allows for postsorting data by actual arrival time at the experiment so that the overall time resolution of the experiment is uncompromised. In these auxiliary experiments, the roles of pump and probe are often reversed relative to the main experiment. A frequently encountered case is one in which the arrival time of the X-ray beam must be compared with that of a conventional femtosecond laser system that operates in or near the visible part of the spectrum. One popular solution to this problem is to use a small portion of the X-ray pulse to transiently change the optical properties of a thin material. These changes are measured by the transmission or reflection of a spectrally chirped optical pulse derived from a split-off portion of the conventional laser system. Here chirped means simply that the pulse is stretched in time so that the arrival time of the pulse on the thin material varies over the fairly broad set of wavelengths that compose the femtosecond laser pulse. A spectrograph set to measure the pulse after interaction with the thin material can then probe the time-dependent reflectivity over a substantial temporal range in a single shot (6, 7). As an alternative to using chirped pulses, a similar outcome can be achieved using a cross-beam geometry (5, 8, 9). Shot-by-shot diagnostics are also used to correct for other types of uncontrolled fluctuations, most often related to the spectrum, intensity, and pointing of the beam.

General scheme of a time-resolved experiment



Irreversible Phase Transition

